Journal of Solid State Chemistry **144,** 423–429 (1999)
Article ID jssc.1999.8191, available online at http://www.idealibrary.com on IDEAL®

Point Defect Energies for Strontium Titanate: A Pair-Potentials Study

Jill Crawford[1] and Patrick Jacobs

Department of Chemistry, The University of Western Ontario, London, Ontario, Canada N6A 5B7

Received August 5, 1998; in revised form January 26, 1999; accepted February 5, 1999

A crystal potential has been derived for strontium titanate and used to calculate the intrinsic defect properties of the room temperature cubic phase. Interactive potentials for a number of uni-, di-, tri-, and tetra-valent metal ions with O^{2-}, Sr^{2+}, and Ti^{4+} has been derived by well-tried methods, using HFSCF calculations of the ionic charge densities and the conserved density approximation. Kinetic energy, exchange, and correlation contributions to the total interaction energy are approximated by the corresponding contributions to an electron gas of the same charge density as the sum of the two SCF ionic charge densities at each separation *R*. These impurity–host lattice potentials are then used to calculate the solubility of these ions in cubic $SrTiO_3$ as well as the possible mobility of these substituents.

Key Words: **strontium titanate; ferroelectrics; computer simulation; radioactive waste.**

1. INTRODUCTION

Strontium titanate ($SrTiO_3$) is an insulator at room temperature but may be made semiconducting at elevated temperatures by inducing nonstoichiometry or by doping (1, 2). It was the first ternary oxide found to display superconductivity (3). At room temperature it has the cubic perovskite structure, but at lower temperatures it undergoes phase transitions to tetragonal (108 K), orthorhombic (65 K), and rhombohedral (35 K) phases (4). The first objective of this investigation was to develop a crystal potential for cubic $SrTiO_3$ and then to use it to calculate defect energies for the pure perovskite and for a range of cation substituents. The results of this study are reported in this paper. A second objective was to calculate the phonon dispersion in $SrTiO_3$ and in particular to see if it was possible to reproduce the mode softening which occurs at the *R* point in the Brillouin zone and which is the driving force for the structural phase transition at 108 K (5–7). The calculation of phonon frequencies is a very sensitive test of shell-model parameters and particularly so for materials with structural instabilities. We consider the ability to reproduce the soft-mode frequency at room temperature a necessary first step in seeing if a shell-model could predict correctly the structures of strontium titanate at lower temperatures. This challenging problem is reserved for a future investigation and the present paper is concerned with defect energies at room temperature. Our prime interest here was to investigate the solubility and mobility of foreign cations in $SrTiO_3$ in view of the possible use of titanates as host materials in radioactive waste disposal. A shell-model calculation of defect energies in $SrTiO_3$ has been reported recently by Akhtar *et al.* (8), but their emphasis lies mainly on the semiconducting properties of $SrTiO_3$.

[1] Present address: Lambton College of Technology, Sarnia, ON, Canada N7S 6K4.

2. THE CRYSTAL POTENTIAL

Our starting point in determining a crystal potential for $SrTiO_3$ and also the impurity ion–host crystal interactions was the calculation of the interaction energy between pairs of ions using the conserved density approximation (9), in which the charge densities of the individual ions are calculated by an atomic SCF program (either in free space or in a simulated crystal field) and the charge density of the interacting species ρ_{12} is then taken to be the sum of the charge densities ρ_1, ρ_2 in the separated ions. In the so-called "electron gas methods" only the Coulomb energy is calculated exactly, the kinetic and exchange contributions being taken to be those of an electron gas of density ρ_{12}, with the Rae correction to remove the self-exchange error (10). For the short-range correlation approximate, formulas of Gordon and Kim (11) or Brual and Rothstein (12) are used. This calculated repulsive interaction was generally fitted to the usual Born–Mayer form

$$\phi_{ij}(R) = D_{ij}\exp(-R/\rho_{ij}), \qquad [1]$$

though in several instances a double-exponential potential

$$\phi_{ij}(R) = D_{ij}\exp(-R/\rho_{ij}) + F_{ij}\exp(-R/\sigma_{ij}) \qquad [2]$$

0022-4596/99 $30.00

gave a much better fit to the calculated interactions and was therefore used instead.

Since no fitting to crystal properties is possible for the cation–cation interactions the calculated potentials were used directly. For several of the metal–oxide potentials (specifically O^{2-} with Ca^{2+}, Mg^{2+}, Sr^{2+}, Ba^{2+}, Fe^{2+}, Co^{2+}, Ni^{2+}, Mn^{2+}) it was possible to refine the calculated potential parameters by comparing calculated and experimental values of crystal properties (13); for the remaining O^{2-}, M^{n+} interactions the calculated potentials were used directly. Potential parameters used for all the required impurity interactions are given in Tables 1 and 2. For many of the metal ion–metal ion interactions it was necessary to introduce a Van der Waals-like term $-C_{ij}/R^6$ on the right-side of Eq. [1] or [2] in order to fit the calculated interaction energies. The values of C_{ij} in the tables are not be taken as serious estimates of the long-range correlation in these interactions but merely as necessary parameters in the fitting of the calculated interaction energies. An example of the results of this fitting procedure (for the Sr^{2+}–U^{4+} interaction) is given in Fig. 1. The double exponential form and the inclusion of the $-C_{ij}/R^6$ term result in an excellent fit over $2\frac{1}{2}$ decades, which is greater than that usually obtained in fitting electron-gas calculation to the Born–Mayer form Eq. [1]. The only exception to the above procedure was the O^{2-}–O^{2-} interaction for which the Born–Mayer parameters calculated by Catlow (14) were used, together with a Van der Waals $-C_{ij}/R^6$ term, the value of C_{ij} being fixed at 20.37 eV Å^6 during refinement of the $SrTiO_3$ potential by fitting to structural, elastic, and dielectric properties. No phonon frequencies were used at this stage. The $SrTiO_3$ potential parameters used in the defect calculations are given in Table 3. The shell-model parameters were obtained from previous work on SrO and TiO_2 (13). Calculated and

TABLE 1
Impurity Ion–Host Ion Potential Parameters: Repulsive Interaction of the Born–Mayer Form

Interaction	D_{ij}/eV	ρ_{ij}/Å	C_{ij}/eV Å^6
Sr^{2+}–Cs^{+}	8047.8	0.28868	112.88
Sr^{2+}–Ca^{2+}[a]	9109.2	0.24234	51.469
Sr^{2+}–Mn^{2+}	10043.0	0.22827	0.0
Sr^{2+}–Fe^{2+}	10723.0	0.22552	0.0
Sr^{2+}–Co^{2+}	11424.0	0.22286	0.0
Sr^{2+}–Ni^{2+}	12144.0	0.22031	0.0
Sr^{2+}–Al^{3+}	11982.0	0.20086	19.553
Sr^{2+}–La^{3+}	12170.0	0.26047	97.295
Sr^{2+}–Ru^{4+}	11036.0	0.24249	10.941
Sr^{2+}–Zr^{4+}	14556.0	0.23213	53.067
Sr^{2+}–Mo^{4+}	8969.5	0.24830	0.0
Ti^{4+}–Cs^{+}	9770.9	0.20670	63.294
Ti^{4+}–Ca^{2+}	12430.0	0.25953	29.670
Ti^{4+}–Fe^{2+}	16198.0	0.18824	4.1116
Ti^{4+}–Co^{2+}	18129.0	0.18366	2.5113
Ti^{4+}–Ni^{2+}	19738.0	0.18052	2.5366
Ti^{4+}–Al^{3+}[a]	20055.0	0.15369	4.3254
Ti^{4+}–La^{3+}	14834.0	0.23160	70.482
Ti^{4+}–Zr^{4+}[a]	18075.0	0.20126	39.664
O^{2-}–Ca^{2+}[a]	1539.9	0.32328	0.0
O^{2-}–Mn^{2+}	2161.1	0.27952	0.0
O^{2-}–Fe^{2+}	2421.2	0.27345	0.0
O^{2-}–Co^{2+}	2714.1	0.26005	0.0
O^{2-}–Ni^{2+}	2810.8	0.25399	0.0
O^{2-}–Al^{3+}[a]	1460.3	0.29912	0.0
O^{2-}–La^{3+}[a]	2993.7	0.31510	0.0
O^{2-}–U^{4+}[a]	1071.3	0.39707	0.0

[a] Ref. (13).

TABLE 2
Impurity Ion–Host Ion Potentials: Double Exponential Repulsive Potential, Eq. [2]

Interaction	D_{ij}/eV	ρ_{ij}/Å	F_{ij}/eV	σ_{ij}/eV	C_{ij}/eV Å^6
Sr^{2+}–U^{4+}	59002.0	0.18442	3163.3	0.34053	148.45
Ti^{4+}–Mn^{2+}	20419.0	0.18863	33.499	0.44013	3.14
Ti^{4+}–U^{4+}[a]	3440.4	0.32182	72749.0	0.16425	114.14
Ti^{4+}–Ru^{4+}[a]	2336.6	0.25814	17573.0	0.18207	13.355
Ti^{4+}–Mo^{4+}[a]	23917.0	0.17498	1764.7	0.28142	24.840
O^{2-}–Cs^{+}[a]	1910.3	0.33187	80024.0	0.13275	35.404
O^{2-}–Ru^{4+}[a]	302.68	0.41629	4374.3	0.23322	0.0
O^{2-}–Mo^{4+}[a]	4830.5	0.24124	316.03	0.41379	0.0

[a] Ref. (13).

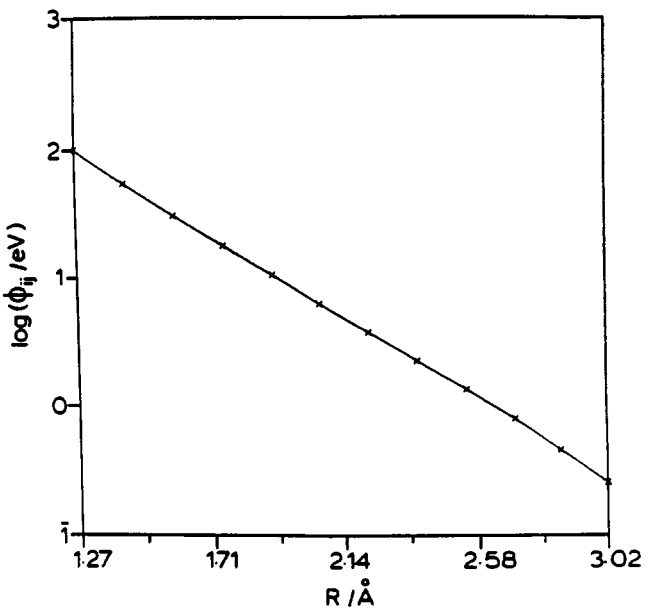

FIG. 1. Representation of the calculated Sr^{2+}–U^{4+} interaction by the double exponential repulsive potential, Eq. [2], plus an attractive term of Van der Waals form.

TABLE 3a
Born–Mayer Repulsive Potential Parameters for the Host–Lattice Ions

Interaction	D_{ij}/eV	ρ/Å
Sr^{2+}–Sr^{2+}[a]	9949.1	0.2446
Sr^{2+}–Ti^{4+}[a]	12708.1	0.2191
Sr^{2+}–O^{2-}	1805.2	0.3250
Ti^{4+}–Ti^{4+}[a]	16963.1	0.1847
Ti^{4+}–O^{2-}	845.0	0.3770
O^{2-}–O^{2-}	22746.3	0.1490

Note. $C_{ij} = 0$ except for O^{2-}–O^{2-}, for which $C_{33} = 20.37$ eV Å^6.
[a] Ref. (13).

TABLE 3b
Shell-Model Parameters for Strontium Titanate

Ion	Y/|e|	K/eV Å^{-2}
Sr^{2+}[a]	7.468	421.9
Ti^{4+}[a]	− 35.863	30490.0
O^{2-}[a]	− 2.249	24.9

[a] Ref. (13).

TABLE 4
Calculated and Experimental Values of Crystal Properties of $SrTiO_3$

	Calculated	Experimental
Cohesive energy/eV	− 150.0	
Lattice constant/Å		3.9051
c_{11}/GPa	330	316[a]
c_{12}/GPa	162	102[a]
c_{44}/GPa	161	123[a]
ε_s	300.9	301[b]
ε_∞	4.76	5.50[c]

[a] Ref. (15).
[b] Ref. (16).
[c] Ref. (17).

experimental values of crystal properties at 298 K are given in Table 4. The experimental lattice constant was used in these calculations and since the calculated basis strains were less than 0.3%, the structure has been fitted with this accuracy.

3. CALCULATION OF DEFECT ENERGIES: INTRINSIC DEFECTS

The energies of formulation and migration of point defects were calculated by the well-tried two-region strategy initiated by Mott and Littleton and implemented in the computer codes HADES and CASCADE. The methodology has been described fully in the literature (9, 18) so no further description of the technique is necessary here except to mention that the HADES III code was used in this work. This code was modified to accommodate the double exponential repulsive potential, Eq. [2], as was the other Harwell code PLUTO (18) used in the calculation of perfect lattice properties. Tests on the energy of formation of an O^{2-} vacancy for various region I sizes N_1, showed that this energy had converged for values of $N_1 \geq 114$ ions and all calculations were therefore performed with $N_1 \simeq 114$. (It is advisable to include complete symmetry classes and therefore the precise size depends slightly on defect symmetry.) Besides Schottky disorder, Frenkel defects may form on any one of the three sublattices. Table 5 shows the energies of formation of vacancies and interstitials and the defect energies in the saddle-point configurations (Figs. 2 and 3) while Table 6 gives the calculated Schottky and Frenkel defect formation energies (per defect) and the migration energies of vacancies and interstitials. From these values we may calculate the Arrhenius energies for instrinsic diffusion, and these results are given in Table 7. These values indicate that in pure $SrTiO_3$ matter transport proceeds via the migration of oxygen vacancies formed from Schottky defects, as concluded by Paladino *et al.* (19) from their studies of oxygen diffusion in single crystals of $SrTiO_3$. The activation energy for oxygen diffusion has also been determined by Kingery *et al.* (20), Yamaji (21), and Walters and Grace (22), and these four sets of data yield oxygen migration energies ranging from 0.98 ± 0.22 to 1.50 eV. Our calculated value of 0.76 eV lies at the lower end of this range, but if the crystals used had contained trivalent impurity ion (e.g., Al^{3+}) substituting at a Ti^{4+} site, then the experimental migration energy will include a term $E_b/2$, where E_b is the impurity-vacancy binding energy. Akhtar *et al.* (8) suggest that E_b should be rather small (0.15 eV in the case of Al^{3+}) so that our calculated value for oxygen vacancy migration is not inconsistent with the rather scattered experimental data that are sensitive to annealing and dislocation density (19). It also agrees tolerably well with the independent result of 0.65 eV

TABLE 5
Defect Energies for $SrTiO_3$ (in eV)

Ion	U_v	U_i	U_{vsp}	U_{isp}
Sr^{2+}	20.915	− 9.126	25.187	− 9.889
Ti^{4+}	84.950	− 68.051	99.275	− 64.483
O^{2-}	18.280	− 9.987	19.016	− 11.327

Note. U_v is the energy required to move an ion from its normal lattice site to ∞, U_i the energy required to move an ion from ∞ to its interstitial position and U_{vsp}, U_{isp}, are the energies required to move the ion from its lattice or interstitial position to the saddle points shown in Figs. 2 and 3.

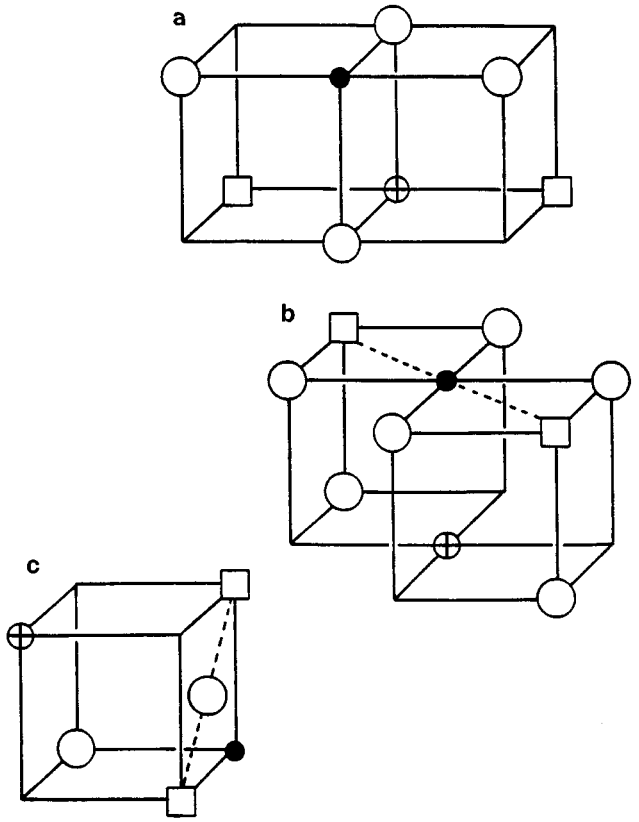

FIG. 2. Saddle-point configurations for vacancy migration in $SrTiO_3$: (a) Sr^{2+}, (b) Ti^{4+}, (c) O^{2-} (Symbols: ● Ti^{4+}, ⊕ Sr^{2+}, ○ O^{2-}).

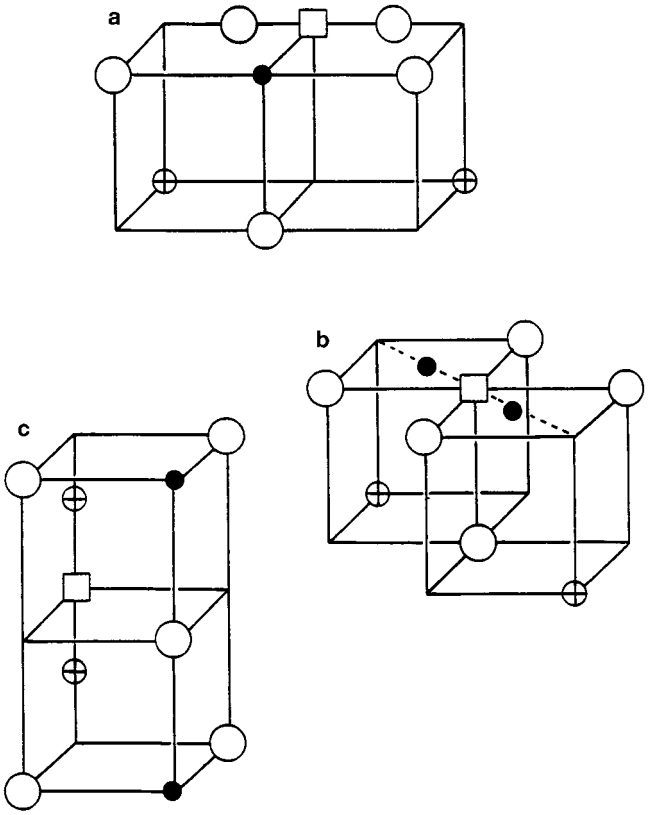

FIG. 3. Saddle-point configurations for ion migration in $SrTiO_3$ by the interstitialcy mechanism: (a) O^{2-}, (b) Ti^{4+}, (c) Sr^{2+}. These figures also enable one to locate the site of the interstitial at edge-centered positions when Ti is at the cube center.

obtained by Akhtar *et al.* (8) using a different crystal potential. The preferred path for oxygen vacancy migration is the linear one along $\langle 110 \rangle$ despite the proximity of the Ti^{4+} ion (Fig. 2c). The calculated Arrhenius energies for cations in Table 7 indicate intrinsic cation diffusion in $SrTiO_3$ to be a rather difficult process. Only Sr^{2+} diffusion, either by cation vacancies on the Sr sublattice or by Sr^{2+} intersitials, would be feasible at very high temperatures. The calculated Arrhenius energy for either a vacancy or an interstitial mechanism is about 6.5 eV (Table 7). Rhodes and Kingery (23) give diffusion activation energies of (4.92 ± 0.99) eV for both Sr^{2+} and Ti^{4+} for dislocation pipe diffusion. For lattice diffusion of Sr^{2+} their value is 6.1 eV. Our calculated value for intrinsic diffusion of Sr^{2+} is somewhat higher than this, but not impossibly so, in view of the extreme practical difficulties involved in measuring diffusion coefficients in the temperature range 1500–1900°C and the further difficulties involved in analyzing experimental diffusion data that has both lattice and dislocation contributions. Identical diffusion rates for Sr^{2+} and Ti^{4+} in dislocations are difficult to understand since one would intuitively expect Ti^{4+} to be much less mobile than Sr^{2+}, as borne out by the calculated values (for lattice diffusion) in Table 7. Ti^{4+} interstitials would be mobile at high temperatures but there seems to be no method of forming these even by doping. Technically, the substitution of four M^{3+} ions at titanium sites could result in a Ti^{4+} interstitial, but this is not an energetically feasible process.

4. DOPED CRYSTALS

The primary focus of the impurity defect work was the calculation of the solubility energies and mobility of various

TABLE 6
Calculated Defect Properties of $SrTiO_3$ (in eV per Defect)

Ion	U_F	ΔU_v	ΔU_i
Sr^{2+}	5.894	4.272	0.763
Ti^{4+}	8.450	14.325	3.568
O^{2-}	4.147	0.757	1.340

Note. The Schottky defect energy U_S (per defect) for $SrTiO_3$ is 2.414 eV. U_F is the Frenkel defect formation energy ΔU_v the migration energy for vacancy motion and ΔU_i the energy required for interstital migration by the interstitialcy mechanism (Figs. 2 and 3).

TABLE 7
Arrhenius Energies (in eV) for Intrinsic Diffusion in $SrTiO_3$

Mobile defect	Schottky vacancy	Frenkel	
		Vacancy	Interstitial
Sr^{2+}	6.40	10.17	6.66
Ti^{4+}	16.45	22.78	12.02
O^{2-}	2.89	4.89	5.48

cations exemplifying those likely to be present in a radioactive waste, namely Cs^+, Ca^{2+}, Mn^{2+}, Fe^{2+}, Co^{2+}, Ni^{2+}, Al^{3+}, La^{3+}, U^{4+}, Zr^{4+}, and Mo^{4+} (25). Accordingly, the only charge compensation considered was by oxygen vacancies or interstitials. It is quite likely that cation solubility will be increased by charge compensation mechanisms involving electrons or holes but this was not examined here in view of the very thorough recent investigation by Akhtar *et al.* (8). The substitution of univalent cations at strontium sites results in the formation of oxygen vacancies to maintain charge neutrality. In conventional Kröger–Vink notation (24)

$$M_2O(c) + 2Sr_{Sr} + 2O_O = 2M'_{Sr} + V_O^{\bullet\bullet} + 2SrO(c) \quad [3]$$

$$2U_{sub} = 2U_c(SrO) + 2U_d(M'_{Sr}) + U_d(V_O^{\bullet\bullet}) - U_c(M_2O), \quad [4]$$

where U_c is the cohesive energy of the substance in parentheses and U_d is the defect energy for (i.e., the energy to form) the species in parentheses. The defect energy U_d was calculated at both a substitutional site and at the saddle point for diffusion by a vacancy mechanism, so that both U_{sub} and ΔU for impurity migration could be calculated, and these values are recorded in Table 8. For isovalent substitutional ions, M^{2+} ions at Sr^{2+} sites or M^{4+} ions at Ti^{4+} sites, no charge compensation is necessary, but the migration energies by a vacancy mechanism were calculated since cation vacancies on either cation sublattice can be formed by substitution of M^{3+} ions at Sr^{2+} sites.

$$MO(c) + Sr_{Sr} = M_{Sr} + SrO(c) \quad [5]$$

$$U_{sub} = U_d(M_{Sr}) + U_c(SrO) - U_c(MO) \quad [6]$$

$$MO_2(c) + Ti_{Ti} = M_{Ti} + TiO_2(c) \quad [7]$$

$$U_{sub} = U_d(M_{Ti}) + U_c(TiO_2) - U_c(MO_2). \quad [8]$$

Trivalent ions may substitute at either strontium or titanium sites. At strontium sites charge compensation may involve oxygen interstitials or strontium vacancies or electrons (reduction). At titanium sites charge compensation occurs by the formation of oxygen vacancies, or electron holes (oxidation). The last possibility is self-compensation when equal numbers of the trivalent ion substituent on strontium and on titanium sites.

TABLE 8
Calculated Defect Energies U_{sub} (in eV per Defect) for the Solution of Metal Oxides in $SrTiO_3$, Classified According to the Mechanism of Charge Compensation

	Impurity	U_{sub}/eV	ΔU/eV
Charge compensation by $V_O^{\bullet\bullet}$			
M^+ on Sr site, Eq. [4]	Cs^+	1.76	25.5
M^{3+} on Ti site, Eq. [14]	Al^{3+}	5.52	96.2
	La^{3+}	5.27	97.6
Charge compensation by O_i''			
M^{3+} on Sr site, Eq. [10]	Al^{3+}	12.04	17.2
	La^{3+}	3.38	26.6
Charge compensation by V''_{Sr}			
M^{3+} on Sr site, Eq. [12]	Al^{3+}	10.32	17.2
	La^{3+}	1.66	26.6
Self-compensation			
M^{2+} on Sr site, Eq. [6]	Ca^+	0.99	24.4
	Mn^{2+}	2.82	21.8
	Fe^{2+}	3.32	18.9
	Co^{2+}	4.34	20.4
	Ni^{2+}	5.06	20.4
M^{4+} on Ti site, Eq. [8]	Mo^{4+}	1.82	101.2
	Ru^{4+}	3.10	98.4
	Zr^{4+}	5.89	100.7
	U^{4+}	7.14	100.2
M^{3+} on Sr and Ti sites, Eq. [16]	Al^{3+}	1.92	17.2[a]
	La^{3+}	−0.63	26.6[a]

Note. ΔU is the calculated energy in eV for the migration of the substituting cation by a vacancy mechanism (on the same sublattice). In each case, U_{sub} refers to the process defined in the equation listed.
[a] On the Sr sublattice.

$$M_2O_3(c) + 2Sr_{Sr} = 2M^{\bullet}_{Sr} + O_i'' + 2SrO(c) \quad [9]$$

$$2U_{sub} = 2U_d(M^{\bullet}_{Sr}) + U_d(O_i'') + 2U_c(SrO) - U_c(M_2O_3) \quad [10]$$

$$M_2O_3(c) + 2Sr_{Sr} = 2M^{\bullet}_{Sr} + V''_{Sr} + 3SrO(c) \quad [11]$$

$$2U_{sub} = 2U_d(M^{\bullet}_{Sr}) + U_d(V''_{Sr}) + 3U_c(SrO) - U_c(M_2O_3) \quad [12]$$

$$M_2O_3(c) + 2Ti_{Ti} + O_O = 2M'_{Ti} + V_O^{\bullet\bullet} + 2TiO_2(c) \quad [13]$$

$$2U_{sub} = 2U_d(M'_{Ti}) + U_d(V_O^{\bullet\bullet}) + 2U_c(TiO_2) - U_c(M_2O_3) \quad [14]$$

$$M_2O_3(c) + Sr_{Sr} + Ti_{Ti} = M^{\bullet}_{Sr} + M'_{Ti} + SrTiO_3(c) \quad [15]$$

$$2U_{sub} = U_d(M^{\bullet}_{Sr}) + U_d(M'_{Ti}) + U_c(SrTiO_3) - U_c(M_2O_3). \quad [16]$$

The substitutional energies per defect, U_{sub}, and activation energies for vacancy migration ΔU (on the same sublattice) are given in Table 8, according to the mechanism of charge compensation. The cohesive energies required in these calculations are given in the Appendix.

Cs^+ was the only univalent ion examined and a value of $U_{sub} = 1.76$ eV is in line with the results of Akhtar *et al.* (8) for Li^+ to Rb^+ (0.71–2.55 eV). These authors also showed that for univalent ions substituting on a Sr^{2+} site with charge compensation by $V_O^{\bullet\bullet}$ (Eq. [3]) is preferred to either charge compensation by holes or substitution on a Ti^{4+} site with $V_O^{\bullet\bullet}$ compensation.

Substitution of divalent M^{2+} ions occurs at strontium sites without the need for charge-compensating defects. The solution energies range from 1 to 5 eV and increase with the mismatch in ionic radii, as shown in Fig. 4. Four modes of solution were examined for the trivalent ions Al^{3+} and La^{3+}. The results in Table 8 show that a clear preference for

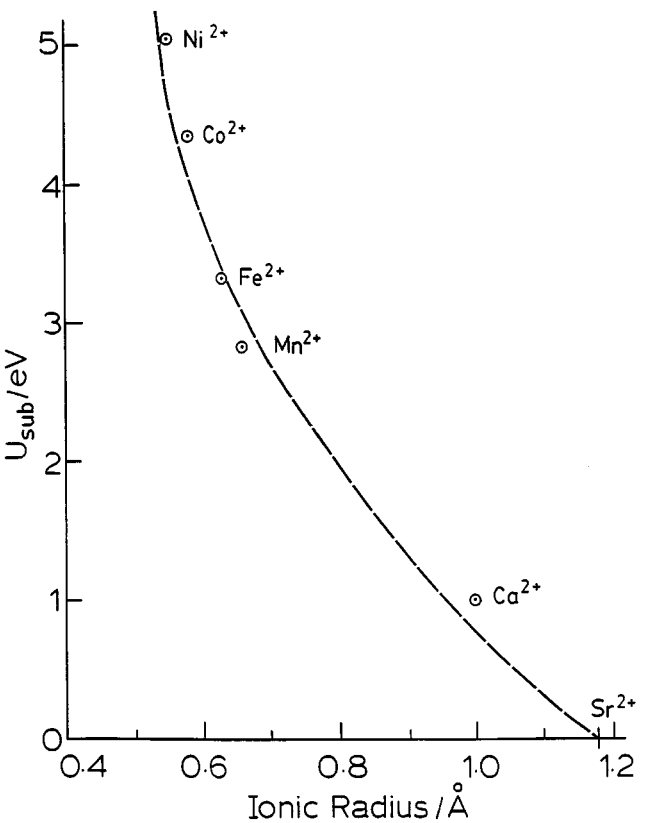

FIG. 4. Plot of U_{sub} (in eV) against ion radius for divalent-cation substituents.

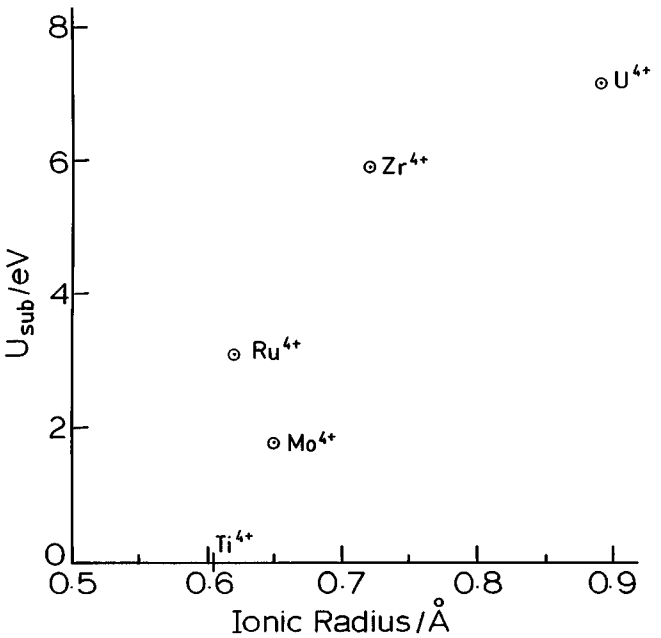

FIG. 5. Plot of U_{sub} in eV ion radius for tetravalent-cation substituents.

self-compensation exists. However, we did not examine the possibility of reduction,

$$M_2O_3(c) + 2Sr_{Sr} = 2M^{\bullet}_{Sr} + \tfrac{1}{2}O_2(g) + 2e' + 2SrO(c), \quad [17]$$

which might give lower solution energies for some trivalent oxides. As expected, the tetravalent cations substitute on titanium sites and again the solution energy of MO_2 increases with the mismatch between the ionic radii of substituent and host lattice cation (Fig. 5). The calculated migration energies are all very high, indicating a high degree of immobilization for any dissolved foreign ions. Although these results refer to 298 K, the values are so large that this conclusion is expected still to hold at the higher temperatures of practical interest.

5. CONCLUSIONS

This work has demonstrated once again the usefulness of computer simulation methods in materials science, particularly in solubility problems and the elucidation of transport mechanisms. It was intended as a first step toward the investigation of the possible use of minerals containing the titanate unit TiO_3^{2-}. One would not in practice use $SrTiO_3$ in radioactive waste disposal but rather a mineral such as sphene (Ca Ti SiO_5) (26), which also contains corner-shared TiO_6^{2-} octahedra, probably incorporated in a glass. The present work has indicated the great versatility and potential use of the alkaline earth titanates in acting as hosts for a great variety of metal oxides. This is because of the

existence of two cation sublattices with metal charges of 2+ and 4+ and their ability to undergo both oxidation and reduction (8). Any dissolved metal ions would diffuse extremely slowly, a necessary requirement in any material intended to immobilize radioactive waste.

APPENDIX

Cohesive energies in eV of some metal oxides.

Al_2O_3	−160.21
CaO	−36.48
CoO	−42.88
Cs_2O	−21.57
FeO	−41.34
La_2O_3	−131.58
MnO	−40.70
MoO_2	−114.47
NiO	−43.82
RuO_2	−118.56
SrO	−34.35
TiO_2	−109.89
UO_2	−102.13
ZrO_2	−105.03

ACKNOWLEDGMENT

Research support from the Natural Sciences and Engineering Research Council of Canada (to P.W.M.J.) is gratefully acknowledged.

REFERENCES

1. N. H. Chan, R. K. Sharma, and D. M. Smyth, *J. Electrochem. Soc.* **128,** 1762 (1981).
2. N. G. Eror and U. Balachandran, *J. Am. Ceram. Soc.* **65,** 426 (1982).
3. C. S. Koonce, M. H. Cohen, J. F. Schooley, W. E. Hosler, and E. R. Pfeiffer, *Phys. Rev.* **163,** 380 (1967).
4. "Landolt–Börnstein," New Series, Group III (K.-H. Hellwege, Ed.), Vol. 7, part e, pp. 134–135. Springer-Verlag, Berlin, 1976.
5. P. A. Fleury, J. F. Scott, and J. M. Worlock, *Phys. Rev. Lett.* **21,** 16 (1968).
6. G. Shirane and Y. Yamada, *Phys. Rev.* **177,** 858 (1969).
7. W. G. Stirling, *J. Phys. C* **5,** 2711 (1972).
8. M. Akhtar, Z. Akhtar, R. A. Jackson, and C. R. A. Catlow, *J. Am. Ceram. Soc.* **78,** 421 (1995).
9. P. W. M. Jacobs, *in* "Diffusion in Materials" (A. L. Laskar, J. L. Bocquet, G. Brébec, and C. Monty, Eds.), p. 203. Kluwer, Dordrecht, 1990.
10. A. I. M. Rae, *Mol. Phys.* **29,** 467 (1975).
11. R. G. Gordon and Y. S. Kim, *J. Chem. Phys.* **56,** 3122 (1972).
12. G. Brual and S. M. Rothstein, *J. Chem. Phys.* **69,** 1177 (1978).
13. C. S. Vempati and P. W. M. Jacobs, *Cryst. Lat. Def. Amorph. Mater.* **10**(9), 19 (1983). [See also unpublished work by the authors]
14. C. R. A. Catlow, *Proc. R. Soc. London A* **353,** 533 (1977).
15. R. O. Bell and G. R. Rupprecht, *Phys. Rev.* **129,** 90 (1963).
16. T. Mitsui and W. B. Westphal, *Phys. Rev.* **124,** 1354 (1961).
17. S. B. Levin, N. J. Field, F. M. Plock, and L. Merker, *J. Opt. Soc. Amer.* **45,** 737 (1955).
18. C. R. A. Catlow and W. C. Mackrodt, *in* "Computer Simulation of Solids" (C. R. A. Catlow and W. C. Mackrodt, Eds.), Chap. 1. Springer-Verlag, Berlin, 1982.
19. A. E. Paladino, L. G. Rubin, and J. S. Waugh, *J. Phys. Chem. Solids* **27,** 391 (1965).
20. W. D. Kingery, J. Pappis, M. E. Doty, and D. C. Hill, *J. Am. Ceram. Soc.* **42,** 393 (1959).
21. A. Yamaji, *J. Am. Ceram. Soc.* **58,** 152 (1975).
22. L. C. Walters and R. E. Grace, *J. Phys. Chem. Solids* **28,** 245 (1967).
23. W. H. Rhodes and W. D. Kingery, *J. Am. Ceram. Soc.* **49,** 531 (1966).
24. J. Phillibert, "Atom Movements: Diffusion and Mass Transport in Solids" (transl. S. J. Rothman), Chap. 6, Appendix II, p. 241. Les Éditions de Physique, Paris, 1991.
25. E. R. Ringwood, S. E. Kesson, N. G. Ware, W. Hibberson, and A. Major, *Geochem. J.* **13,** 141 (1979).
26. A. Gallego-Sala, A. V. Chadwick, K. M. Kennedy, K. D. Becker, and D. Niemeier, "8th Europhysical Conference On Defects in Insulating Materials," Keele, UK, 6–11 July 1998; *Rad. Eff. Def. Solids*, to be published.